Human Movement Science 66 (2019) 645–658

Contents lists available at ScienceDirect

Human Movement Science

journal homepage: www.elsevier.com/locate/humov

Full Length Article

Kinetic analysis of oxygen dynamics under a variable work rate

Alexander Artiga Gonzalez[a,*], Raphael Bertschinger[b], Fabian Brosda[a], Thorsten Dahmen[a], Patrick Thumm[b], Dietmar Saupe[a]

[a] Dept. of Computer and Information Science, University of Konstanz, Fach 697, 78457 Konstanz, Germany
[b] Sensorimotor Performance Lab, Department of Sport Science, University of Konstanz, 78457 Konstanz, Germany

ARTICLE INFO

Keywords:
Mathematical modeling
Simulation
Oxygen dynamics
Variable work rate

ABSTRACT

Measurements of oxygen uptake are central to methods for the assessment of physical fitness and endurance capabilities in athletes. Two important parameters extracted from such data of incremental exercise tests are the maximal oxygen uptake and the critical power. A commonly accepted model of the dynamics of oxygen uptake during exercise at a constant work rate comprises a constant baseline oxygen uptake, an exponential fast component, and another exponential slow component for heavy and severe work rates. We have generalized this model to variable load protocols with differential equations that naturally correspond to the standard model for a constant work rate. This provides the means for predicting the oxygen uptake response to variable load profiles including phases of recovery. The model parameters have been fitted for individual subjects from a cycle ergometer test, including the maximal oxygen uptake and critical power. The model predictions have been validated by data collected in separate tests. Our findings indicate that the oxygen kinetics for a variable exercise load can be predicted using the generalized mathematical standard model. Such models can be applied in the field where the constant work rate assumption generally is not valid.

1. Introduction

Physiological quantities, such as heart rate, lactate concentration, or respiratory gas exchange, are important parameters for assessing the performance capabilities of athletes in competitive sports, in particular in endurance sports. Respiratory gas exchange is a valuable source of information since it allows for a non-invasive, continuous, and precise measurement of the gross oxygen uptake and carbon dioxide output of the whole body.

Characteristic responses to specific load profiles in different intensity domains have been subject of research effort in recent years (Jones & Poole, 2005; Poole & Jones, 2012). The most distinctive parameters in the description of $\dot{V}O_2$ kinetics are the highest attainable oxygen uptake ($\dot{V}O_{2\max}$), the steady-state level with submaximal load, and the rate of increase in $\dot{V}O_2$ at the transition to a higher load level. Basically, the oxygen uptake mechanism may be viewed as a combination of first-order control systems (Özyener, Rossiter, Ward, & Whipp, 2001; Whipp & Rossiter, 2005). Thus the responses to step-shaped load profiles are often described with exponential functions that serve as a regression to the measured data.

In particular, for endurance sports like cycling, the mathematical models for the power demand due to mechanical resistance are well understood. However, the individual power supply model of an athlete is the bottleneck that has hindered the design of an individual adequate feedback control system to guide him/her to perform a specific task, such as to find the minimum-time pacing in a race on a hilly track (Dahmen, 2012). For such purposes, a dynamic model for the prediction of gas exchange rates in response to

* Corresponding author.
E-mail address: alexander.artiga-gonzalez@uni-konstanz.de (A. Artiga Gonzalez).

http://dx.doi.org/10.1016/j.humov.2017.08.020

Available online 14 September 2017
0167-9457/ © 2017 Elsevier B.V. All rights reserved.

load profiles given by a particular race course would be beneficial.

Stirling, Zakynthinaki, and Billat (2008) provided a dynamic model. However, it deviates significantly from several theoretical physiological aspects. E.g., it does not consider separate fast and slow components and any delays in the response to heavy and severe work rates. Moreover, it does not provide a model for the steady state oxygen demand as a function of exercise load, and has not been applied to variable load profiles.

We propose that the first step towards dynamical models for variable loads should be derived from the established models for constant work rate before more general models are considered and can be compared with the former ones. Therefore, in this contribution, we generalize the original model equations to arbitrary load profiles and calibrate and validate them using four load profiles of different characteristics.

A precursor for these tasks was already presented in our recent work (Artiga Gonzalez et al., 2015), which modeled and predicted the oxygen dynamics, however with an overestimation of the slow component. This paper reviews and extends the discussion of our previous study. In particular, we have been able to significantly improve the model and the prediction in the severe work domain where the slow component is most prominent. This further progress has been made possible by including two of the model parameters, namely the maximal oxygen uptake and the critical power, into the optimization procedure instead of using the directly measured values.

2. Previous work

A detailed review and historical account of the mathematical modeling of the $\dot{V}O_2$ kinetics for constant work rate (CWR) has recently been given by Poole and Jones (2012), containing over 800 references. See also Jones and Poole (2005) and, for a clarification, Ma, Rossiter, Barstow, Casaburi, and Porszasz (2010). Therefore, here we only briefly summarize the established model to the extent necessary for an understanding of our generalization, but refer to the above mentioned papers for further explanations and references to the literature.

According to the commonly accepted and widely applied model, the $\dot{V}O_2$ kinetics can be separated into four distinct components.

- The baseline component. This constant component accounts for the oxygen consumption at rest, i.e., for the time prior to the onset of exercise.
- A rapid, initial increase (Phase I). At the start of the exercise, a rapid but small initial increase of $\dot{V}O_2$ occurs and is completed within the first 20 s.
- The primary, fundamental, or fast component (Phase II). This phase is characterized by a (typically larger) exponential increase of $\dot{V}O_2$ with a time constant of 20–45 s. After saturation, and for a given work rate below the critical power, this component represents the required steady-state demand of oxygen.
- A secondary, slow component (Phase III). The slow component occurs only for work rates above the critical power. It brings about an additional increase of $\dot{V}O_2$ to a total that for severe work rates above the critical power is roughly equal to the maximal oxygen consumption, $\dot{V}O_{2\max}$.

Each of the components in Phases I to III are modeled as exponential functions of type

$$A\left(1-\exp\left(-\frac{t-T}{\tau}\right)\right) \tag{1}$$

where time is denoted by t and with different amplitudes A, time delays T, and time constants τ, see Fig. 1. The time constant τ

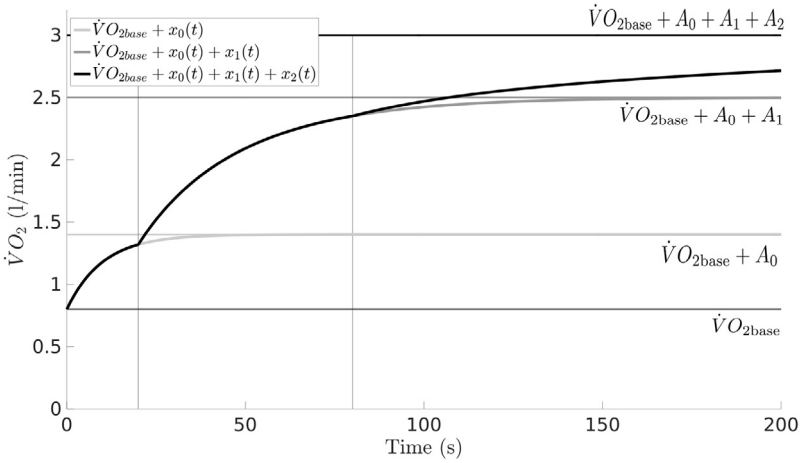

Fig. 1. Steady-state dynamics consisting of a baseline component $\dot{V}O_{2\text{base}}$ together with three exponentially asymptotic functions $x_0(t), x_1(t)$ (fast component), and $x_2(t)$ (slow component) of different amplitudes, decay rates, and delays.

determines the time required for the dynamics of the corresponding component to diminish the difference from the asymptotic amplitude A by a factor of $1-1/e \approx 0.632$. Thus, after a time of 3τ, about 95% of the amplitude A is reached and the corresponding phase is regarded as effectively having reached its final value. It is important to note that the time delay T is intended to imply that only after that time has the oxygen consumption of the corresponding component begun. To complete the model, we therefore employ the Heaviside step function (Ma et al., 2010)

$$H(t) = \begin{cases} 1, & t \geq 0 \\ 0, & t < 0 \end{cases} \tag{2}$$

setting

$$x_k(t) = A_k \; H(t-T_k)\left(1-\exp\left(-\frac{t-T_k}{\tau_k}\right)\right) \tag{3}$$

yielding the complete model in one formula as

$$\dot{V}O_2(t) = \dot{V}O_{2\text{base}} + \sum_{k=0}^{2} x_k(t). \tag{4}$$

Here, $\dot{V}O_{2\text{base}}$ is the baseline component, and the index $k = 0,1,2$ refers to the components of the three phases, which are parametrized by their corresponding amplitudes A_k, time delays T_k, and time constants τ_k. In Phase I there is no delay: $T_0 = 0$. This is the standard form of oxygen dynamics, and is illustrated in Fig. 1.

Phase I typically lasts only a couple of breaths until reaching its target amplitude A_0 and during this short period of time at the onset of exercise there is a large variability in the inter breath gas exchange, making it difficult to fit a model to an individual ventilatory data series (Whipp, Ward, Lamarra, Davis, & Wasserman, 1982). Therefore, many researchers remove that time period from the data and consider only the first, fast response and the second, slow component (Jones and Poole, 2005, page 26). The baseline amplitude would then have to be incremented by the amplitude A_0 to compensate for the deletion of Phase I. In this study we also follow this procedure. Thus, from here on, $\dot{V}O_{2\text{base}}$ refers to the above mentioned baseline component (renamed $\dot{V}O_{2\text{min}}$ and measured directly) plus an estimated add-on accounting for A_0.

In this kinetic model of $\dot{V}O_2$ consumption for a constant work rate, the amplitudes A_k must be chosen adaptively. They depend on the physiological and metabolic condition of the subject and on the applied constant work rate P. Thus, $A_k = A_k(P)$. As a first approximation, the amplitude of the first, fast component can be taken as a linear function of exercise intensity (power), with slope of 9–11 ml/min per Watt of power increase and bounded by $\dot{V}O_{2\text{max}}$ (Poole and Jones, 2012, page 939).

The second, slow component is more complex. It is the sum of two parts. The first part is an increasing function, which seems to start having nonzero values from about the gas exchange threshold up to the value of the critical power P_c, where the sum of all components is still less than $\dot{V}O_{2\text{max}}$. The exact form of this function has not been determined. For power greater than the critical power, the slow component for constant work rate exercise eventually raises the total oxygen consumption up to $\dot{V}O_{2\text{max}}$. Thus, for $P > P_c$, it can be modeled as an affine linear, decreasing function which is the difference between $\dot{V}O_{2\text{max}}$ and the sum of the amplitudes of the baseline and the first, fast component.

This model has been validated with CWR and also incremental exercise, where the slow component is not apparent, or at least not fully apparent. In the following section we propose a concrete parametrized model of the total oxygen consumption following these findings, summarized in Fig. 5.

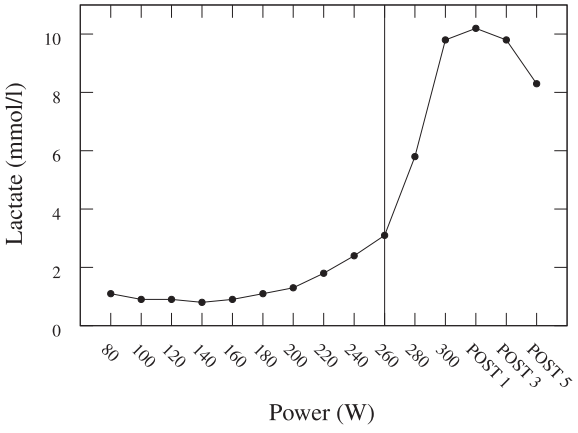

Fig. 2. Example of the method of determining the lactate threshold in the lactate curve for Subject 5.

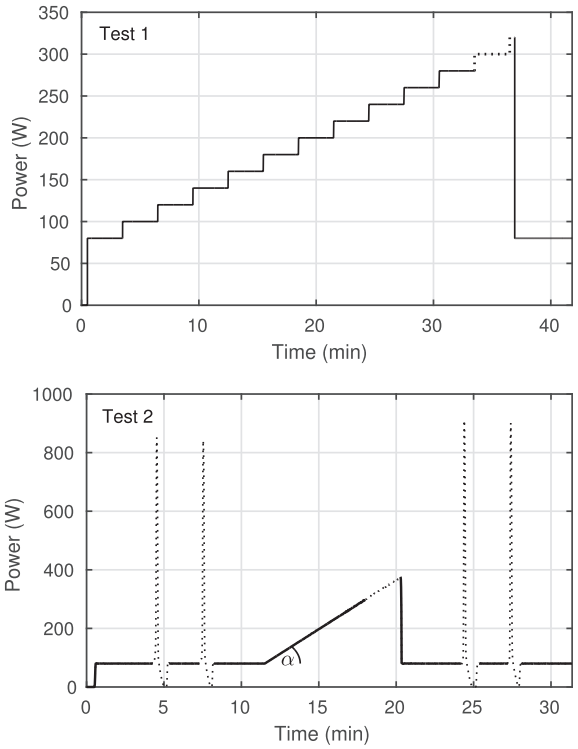

Fig. 3. Test protocols of the first (top) and second (bottom) cycle ergometer test (see text for details). Dashed lines indicate individual variability in maximal power output achieved during the test. The angle α indicates individual variability in the calculated slope of the workload increase.

3. Methods

3.1. Experimental setup

Six healthy subjects (age 37.8 ± 14.8 yrs, height 180.4 ± 10.1 cm, weight 75.2 ± 7.6 kg) with a cycling background ranging from recreational to amateur level gave written informed consent to take part in the study and were thoroughly informed about the testing procedure. The subjects completed four different cycle ergometer (Cylus2, RBM elektronik-automation GmbH, Leipzig, Germany) tests with continuous breath-by-breath gas exchange and ventilation measurements at the mouth (Ergostik, Geratherm Respiratory GmbH, Bad Kissingen, Germany). The first two test protocols were designed to determine a set of physiological parameters of aerobic capacity that will be employed as upper and lower boundaries for the modeling process. The two remaining tests featured varying load profiles in order to comprehensively evaluate the prediction quality of the model.

The following paragraphs describe the four test protocols in detail. See Figs. 3 and 4 for illustrations of the corresponding work rate and road gradient profiles.

Test 1 (see Fig. 3, top).

The experimental procedure commenced with an incremental step test to assess the power output at the anaerobic lactate threshold (*pLT*). *pLT* is needed as a lower boundary for estimating the model parameter P_c. The review by Hill (1993) demonstrates that the anaerobic threshold lies below P_c and therefore justifies the use of *pLT* as a lower limit. The step test started at a workload of 80 W increasing by 20 W every 3 min. In the initial step, the subjects were instructed to choose their preferred cadence between 80–100 rpm and were then instructed to keep the cadence constant in all four trials. The step test was terminated at volitional exhaustion of the subject. After test termination, the subjects recovered actively at 80 W and at or near their self-selected cadence for five minutes. In this test, in addition to gas exchange recordings, blood lactate measurements (Lactate Pro 2, Arkray Factory Inc., Shiga, Japan) were sampled to determine the lactate threshold as described below. Lactate probes from the earlobe (0.3 µl) were taken at the end of every step, at volitional exhaustion of the subject as well as 1, 3, and 5 min after test termination. The "lactate threshold is the exercise intensity that is associated with a substantial increase in blood lactate during an incremental exercise test" (Svedahl & MacIntosh, 2003), hence the lactate threshold was determined as the workload before an increase in lactate concentration of at least 1/10th of the maximal lactate concentration (reached either at the abortion of the test or in the recovery phase) could be observed. The step before this substantial blood lactate increase was chosen as the power at the lactate threshold (*pLT*), see Fig. 2.

To validate this approach, we compared our resulting *pLT* values against seven established methods for detection of the lactate threshold (Baldari & Guidetti, 2000; Bishop, Jenkins, & Mackinnon, 1998; Cheng et al., 1992; Coyle et al., 1983; Dennis, Noakes, & Bosch, 1992; Heck et al., 1985; Morton et al., 1994). The *pLT* values that we adopted in our study are well within one

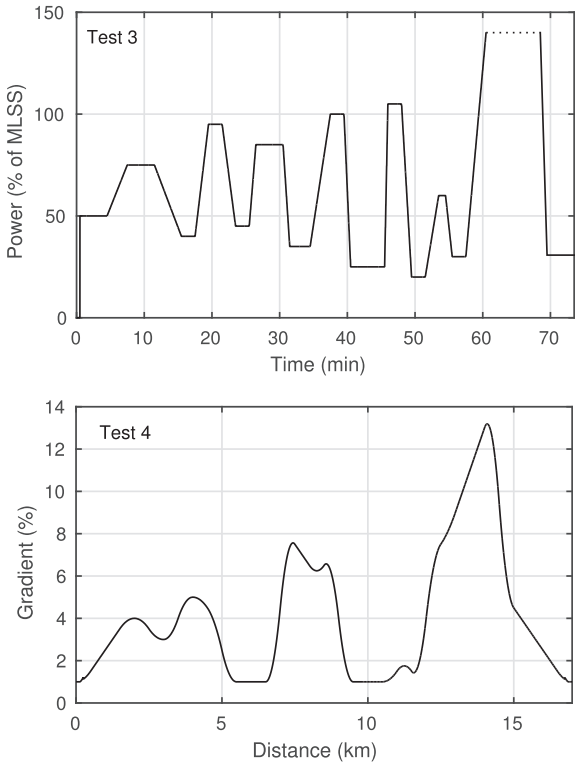

Fig. 4. Test protocols of the third (top) and fourth (bottom) cycle ergometer test (see text for details). The dashed line in Test 3 indicates individual variability of time achieved at 140% of *pLT* workload.

standard deviation of the average of the seven reference values, see Table 1.

Test 2 (see Fig. 3, bottom).

The second ergometer test consisted of four sprints of 6 s duration each and an incremental ramp test. Two sprints were carried out before and two after the ramp test to obtain the subjects' maximal power output and $\dot{V}O_2$ profiles in a recovered and a fatigued state. Before each set of sprints, the subjects pedaled at 80 W for 5 min at their self-selected cadence. The two sprints of each set were separated by 30 s of passive rest and a subsequent 2 min 24 s of active recovery at 80 W. The ergometer load for the sprints was calculated on the basis the subjects' body weight multiplied by a factor of 5, expressed in Newton. Ten seconds before each sprint, the subjects were instructed to increase their cadence gradually in order to obtain their maximal pedaling frequency right at the start of the sprint when the load was applied to the flywheel of the ergometer. The subjects were able to time their effort by a countdown visually presented on a large screen.

In order to obtain approximately the same ramp test time of 10 min for every subject, the end load of the ramp protocol was

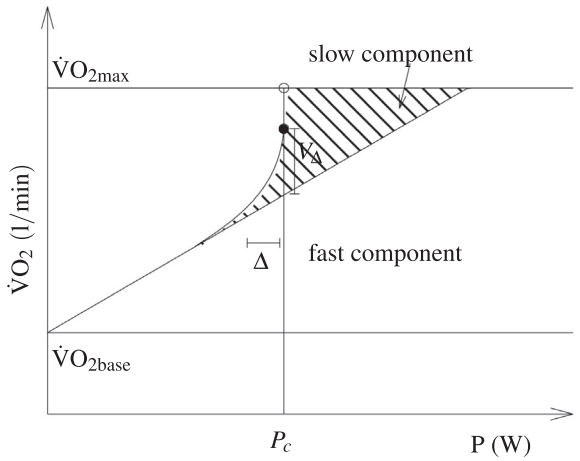

Fig. 5. Model of the steady state oxygen demand for the baseline, fast, and slow components.

Table 1
Comparison of the used power at lactate threshold values (*pLT*, second column) with those from seven established methods for detection of the lactate threshold. For each subject the average and the standard deviations with respect to the seven methods are given in the last two columns. All numbers are in Watts and rounded.

	pLT	Baldari (Baldari & Guidetti, 2000)	Bishop (Bishop et al., 1998)	Cheng (Cheng et al., 1992)	Dennis (Dennis et al., 1992)	Coyle (Coyle et al., 1983)	Heck (Heck et al., 1985)	Morton (Morton et al., 1994)	Average	σ
Subject 1	380	360	382	311	357	369	388	368	362	25
Subject 2	240	260	276	225	253	263	283	236	257	21
Subject 3	200	180	224	194	219	193	215	214	206	16
Subject 4	220	200	226	195	218	203	220	223	212	12
Subject 5	260	220	262	225	258	237	267	259	247	19
Average	260	244	274	230	261	253	275	260	257	16

estimated individually by the highest exercise intensity reached in the incremental step test multiplied by a factor of 1.3. The start load was set to 80 W, hence the increase per minute was obtained by the following formula: (Individual end load of step test in Watt − start load of 80 W)/ 10 min. The workload was increased every second until the subject terminated the test volitionally.

VT_1 was determined visually on the basis of the ramp protocol in Test 2. The method used is described in detail in Beaver, Wasserman, and Whipp (1986). Briefly, plots of VE/VCO_2,VE/VO_2, end-tidal PCO_2 ($PETCO_2$), end-tidal PO_2 ($PETO_2$) and respiratory exchange ratio (*RER*) vs. time were analyzed. The first criterion for VT_1 is an increase in the VE/VO_2 curve after it has declined or stayed constant, without an increase in VE/VCO_2. The second criterion is a slowly rising or constant $PETCO_2$ curve together with a beginning in the rise of the $PETO_2$ curve after it has had a flat or declining shape. The third criterion is a marked increase in *RER* after a horizontal or slowly rising shape. For reasons of simplicity, the lag of the $\dot{V}O_2$ increase with respect to the workload of the ramp test has not been taken into consideration in the determination of VT_1 workload.

$\dot{V}O_{2max}$ was determined as the highest $\dot{V}O_2$ of a 10-value moving average obtained in any of the four tests. In 4 out of 5 subjects, the test with the highest $\dot{V}O_{2max}$ was the ramp test. The other subject reached $\dot{V}O_{2max}$ in the incremental step test.

$\dot{V}O_{2min}$ was determined as the lowest $\dot{V}O_2$ value obtained during the 30 s resting phase in any of the four ergometer tests.

Table 2 summarizes the parameters from direct measurements and the results.

Test 3 (see Fig. 4, top).

In the third test, the subjects had to complete a variable step protocol. The steps varied in load and duration and alternated between low and moderate or severe intensity. The linearly increasing or decreasing intensity between the steps was also varied in time. The intensities were calculated in relation to the *pLT*. In short, the step protocol looked as follows: 4 min at 80 W, 4 min at 75% *pLT*, 2 min at 40% *pLT*, 2 min at 95% *pLT*, 2 min at 45% *pLT*, 4 min at 85% *pLT*, 3 min at 90 W, 2 min at 100% *pLT*, 5 min at 80 W, 2 min at 105% *pLT*, 2 min at 70 W, 1 min at 60% *pLT*, and 2 min at 80 W. Fixed workloads for some intervals were used because the ergometer was not able to handle workloads that were below 40% of *pLT* for some subjects. Subsequently, a constant load all-out exercise at 140% *pLT* followed. This interval lasted from 1.5 to 4.5 min between subjects. The final interval was designed as a recovery ride at 80 W for 5 min.

Test 4 (see Fig. 4, bottom).

For the final "synthetic hill climb test" the ergometer was controlled by our simulator software (Dahmen, Byshko, Saupe, Röder, & Mantler, 2011). The load was defined by a mathematical model (Martin, Milliken, Cobb, McFadden, & Coggan, 1998) to simulate the resistance on a realistic track. The gradient of that track, depicted in Fig. 4, and the subjects' body weight were the major determinants of the load. While maintaining the same cadence as before, the subjects were able to choose their exercise intensity by gear shifting. (On the steepest section most subjects were not able to maintain the cadence even in the lowest gear.)

Before each session the gas analyzers were calibrated with ambient air and a gas mixture of known composition (15% O_2, 5% CO_2 and the balance was N). The flow sensor was calibrated by means of a 3-liter syringe. For an adequate recovery, the test sessions were separated by at least 48 h. The subjects were instructed to visit the laboratory in a fully recovered state and were asked to refrain from intense physical activity two days prior to testing. In all test sessions, the subjects received strong verbal encouragement from the investigators when they were close to their physical limits. During all the experiments, the subjects were aware of the relevant mechanical variables, such as the power and cadence, displayed on a large screen. The cadence was held constant throughout all tests except the sprints in Test 2 and the steep sections (>10% gradient) of Test 4. To obtain a minimal $\dot{V}O_2$ ($\dot{V}O_{2min}$) value, subjects stayed seated for 30 s on the ergometer before the start of each test.

Table 2
Parameters extracted from ergometer tests. The averages are over the five study subjects.

Param.	Unit	Description	Average ± σ
$\dot{V}O_{2min}$	l/min	minimal oxygen uptake	0.354 ± 0.070
VT_1	W	first ventilatory threshold	183 ± 26
$\dot{V}O_{2max}$	l/min	maximal oxygen uptake	4.708 ± 0.873
pLT	W	power at lactate threshold	260 ± 71

Table 3
Summary of parameters for the model of the steady state oxygen demand.

Param.	Unit	Description	Range
P_c	W	critical power	$[pLT, s^{-1}(\dot{V}O_{2max} - V_\Delta - \dot{V}O_{2base})]$
$\dot{V}O_{2base}$	l/min	baseline $\dot{V}O_2$	$[\dot{V}O_{2min}, \dot{V}O_{2max} - V_\Delta - sP_c]$
$\dot{V}O_{2max}$	l/min	maximal $\dot{V}O_2$	$[\dot{V}O_{2base} + sP_c + V_\Delta$, measured value$]$)
s	l/min/W	exercise economy	$[0.25 \cdot P_c^{-1}\dot{V}O_{2max}, P_c^{-1}\dot{V}O_{2max}]$
V_Δ	l/min	ampl. slow comp.	$[0, \dot{V}O_{2max} - \dot{V}O_{2base} - sP_c]$
Δ	W	range slow comp.	$[0, P_c - VT_1]$

3.2. The steady-state oxygen demand model

Following the model assumptions from the literature as summarized in Section 2, we propose a steady state oxygen demand given by a constant baseline component, the first, fast component, and the second, slow component with amplitudes $\dot{V}O_{2base}$, $A_1(P)$, and $A_2(P)$, respectively. The exact form of the slow component for loads below the critical power is not specified in the literature and we propose an exponential function, parametrized by its amplitude and growth rate. In terms of formulas, the amplitudes are

$$A_1(P) = \min(s \cdot P,\ \dot{V}O_{2max} - \dot{V}O_{2base}) \tag{5}$$

$$A_2(P) = \begin{cases} V_\Delta \cdot \exp(-(P_c - P)/\Delta) & P \leqslant P_c \\ \dot{V}O_{2max} - \dot{V}O_{2base} - A_1(P) & P > P_c \end{cases} \tag{6}$$

where s is the slope (or gain) for the fast component (about 9–11 ml/min/W), P_c denotes the critical power, V_Δ is the maximal amplitude of the slow component for exercise load up to critical power, and Δ is the corresponding decay constant that governs the decay of the steady-state slow component as the load is decreased from the critical power. Fig. 5 depicts the graph of the sum of all components in this model.

The parameters for this steady state oxygen demand model were determined by least squares fitting to data from one or more ergometer tests ($\dot{V}O_{2max}$, P_c, $\dot{V}O_{2base}$, s, V_Δ, and Δ, see Table 3). For the fitting procedure, the appropriate search ranges for the parameters are also specified in Table 3. These ranges are based on experimental evidence ($\dot{V}O_{2base}$, Δ) or on constraints of the model. E.g., the upper bound $\dot{V}O_{2max}/P_c$ for the slope s stems from the extreme case where $\dot{V}O_{2base} = 0$ and $\dot{V}O_2(P_c) = \dot{V}O_{2max}$.

We point out that we had previously taken the parameters $\dot{V}O_{2max}$ and P_c for our dynamic model of oxygen consumption directly from the ergometer tests (Table 2) (Artiga Gonzalez et al., 2015). However, we found that the model overestimated the slow component because the parameters as measured directly seemed to be too small or too large for the purpose of the model. Therefore, we propose to determine these parameters also by means of parameter fitting instead of direct (and perhaps inappropriate) measurements.

3.3. Dynamic model of oxygen consumption

Now let us extend the steady state oxygen demand model so that it becomes dynamic, allowing for a variable load profile $P(t)$. The response of the fast and slow components in the case of a constant work rate demand is given by Eq. (1), $A\left(1 - \exp\left(-\frac{t-T}{\tau}\right)\right)$. Note that this function is the solution of the linear ordinary differential equation initial value problem

$$\dot{x} = \tau^{-1}(A - x),\ x(0) = 0 \tag{7}$$

however, delayed by the delay time T or, equivalently, the solution for initial value $x(T) = 0$. This suggests the following equations for the first and second component, $x_1(t)$,$x_2(t)$,

$$\dot{x}_k = \tau_k^{-1}(A_k(P) - x_k),\ x_k(T_k) = 0,\ k = 1,2 \tag{8}$$

defined for times $t \geqslant T_k$ (and setting $x_k(t) = 0$ for $t < T_k$). Here, the power demand is a function of time $P = P(t)$ and the $A_k(P)$,$k = 1,2$, are the steady state amplitudes for the fast and slow components given in Eqs. (5) and (6). The total $\dot{V}O_2$ accordingly is given by

$$\dot{V}O_2(t) = \dot{V}O_{2base} + x_1(t) + x_2(t). \tag{9}$$

These differential equations require the four parameters τ_1, τ_2, T_1, and T_2 that are listed together with their corresponding ranges in Table 4. These ranges are set in accordance with empirical findings reported in the survey article of Jones and Poole (2005).

We remark that the above $\dot{V}O_2$ model does not distinguish between on- and off-transient dynamics, i.e., the $\dot{V}O_2$ demand and time constants are the same regardless of whether the current $\dot{V}O_2$ value is below (on-transient case) or above the $\dot{V}O_2$ demand (off-transient case). There is, however, some evidence for an asymmetry of dynamics in some of the exercise intensity domains, although this has received little attention in the literature (Poole and Jones, 2012, p. 940). For simplicity, in this paper we stay with the symmetric model and leave the modeling of asymmetric dynamics for future research.

Table 4
Parameters for the dynamic model of oxygen consumption. Together with the model for steady state oxygen demand there are 10 parameters to be estimated.

Param.	Unit	Description	Range
τ_1	s	time constant fast comp.	[20,45]
τ_2	s	time constant slow comp.	[60,300]
T_1	s	time delay fast comp.	[0,20]
T_2	s	time delay slow comp.	[30,240]

3.4. Data preprocessing

In order to estimate the ten parameters of the dynamic model given by Eqs. 5, 6, 8 for a particular subject, the data series of the time-stamped values of power produced and the resulting breath-by-breath oxygen consumption are required for exercise intensities ranging from moderate to severe. These time series from ergometer laboratory experiments are typically very noisy, have different sampling rates for $\dot{V}O_2$ and power, and the samples may be irregularly spaced.

Therefore, a combined smoothing and resampling operator has to be applied before parameter estimation. In this study we have used the standard Gaussian smoothing filter with kernel $(\sigma\sqrt{2\pi})^{-1}\exp(-0.5t/\sigma^2)$ and $\sigma = 20$ s for respiratory and power measurements. The filter was applied at time instants uniformly spaced at 1 s intervals. Fig. 6 gives an example of measured time series and their smoothed and resampled version.

3.5. Parameter estimation

The parameter estimation was done by least squares fitting, minimizing the mean-squared error between the computed model values and the (smoothed) $\dot{V}O_2$ data. Testing has shown that fitting versus the smoothed $\dot{V}O_2$ data produced better results than against noisy measured data. Non-linear least squares fitting may suffer from the presence of many local minima. Thus, commonly applied optimization algorithms like the downhill simplex method typically get stuck in these, and the results depend greatly on the choice of the initial parameters. Therefore, we adopted a genetic algorithm from MATLAB® (MATLAB, 2017a), which provided better minima by use of its stochastic elements. The genetic algorithm does not depend on a well chosen starting point but is reliant on population size and size of the search space given by the upper and lower bounds of the parameters.

The model values were computed by solving the differential equations in MATLAB® with the *ode45* function (MATLAB, 2017b) which is a solver for nonstiff differential equations based on the Dormand-Prince method. For proper solutions, the values for absolute and relative tolerance for the ode solver were set to 10^{-6}. The settings for the genetic algorithm (*ga*) are described in Table 5. Computations were done in MATLAB® in parallel with 16 workers on a setup with two *Intel® Xeon® E5-2640 v3 2.60 GHz* with 192 GB RAM, *Debian Jessie* operating system and MATLAB® 2016a.

Average computation time was 3547 ± 1792 seconds with an average of 69 ± 15 iterations.

3.6. Model validation

We calculated the model parameters for each ergometer test of each participating subject. To express the quality of the fit of the model to the data, we computed the root-mean-square differences. To validate the predictive power of the model, we selected Test 3 for each subject for parameter fitting, and used the other tests for comparing the model predictions of oxygen consumption with the

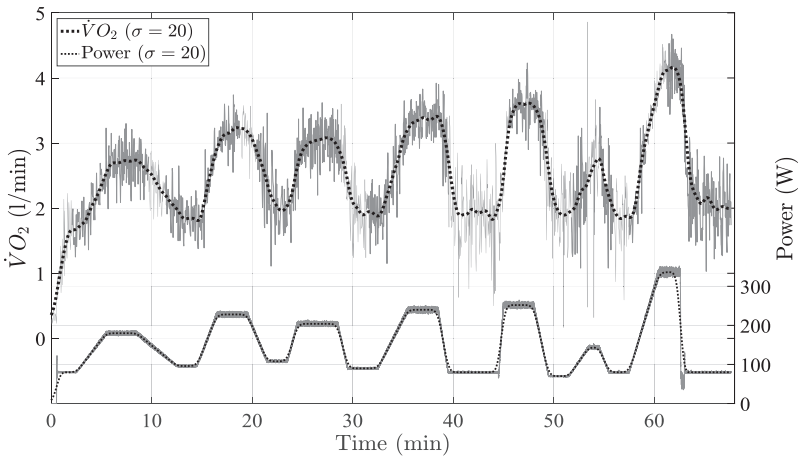

Fig. 6. Data filtering for ventilatory and power data.

Table 5
Settings for the genetic algorithm. Model parameters are normalized between 0 and 1.

PopulationSize	1024
InitialPopulationRange	[0...0;1...1]
MaxStallGenerations	20
ConstraintTolerance	10^{-5}
FunctionTolerance	10^{-5}
NonlinearConstraintAlgorithm	penalty

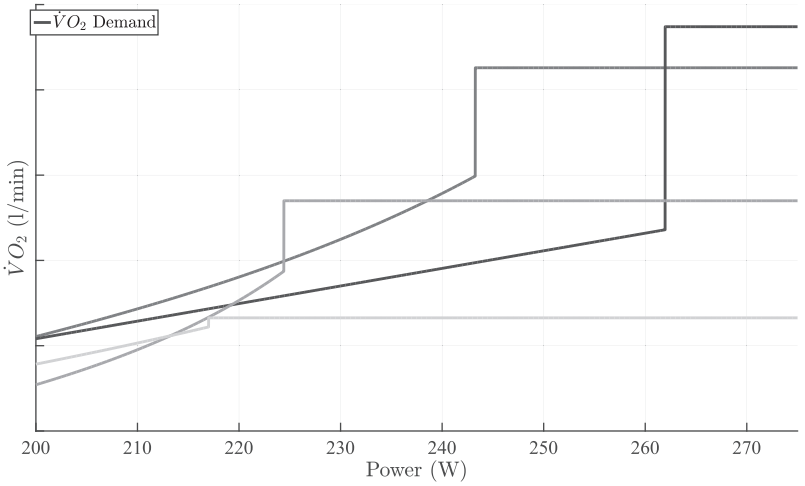

Fig. 7. Closeup of the fitted models of steady state oxygen demand for subjects 2 to 5 (compare with Table 6). The discontinuity at the critical power P_c and the exponential parts of the slow component below critical power for subjects 2 and 3 are clearly visible.

measured values.

4. Results

The $\dot{V}O_2$ model as given by Eqs. 5, 6, 8, 9 was fitted with the least squares method to the data for all four tests and five subjects, resulting in 20 sets of model parameters. The corresponding model errors were calculated by solving the initial value problems in Eq. (8) and summing up the components according to Eq. (9). The resulting model errors are given in Table 7.

Overall, the average $\dot{V}O_2$ modeling RMS error was 0.09 ± 0.03 l/min amounting to an mean absolute percentage error of 3.1%. Fig. 8 illustrates the $\dot{V}O_2$ and power data, and the fitting result for Subject 2, whose average RMS error is the median of the errors for subjects.

In the modeling phase, we found that Test 1 performed best, with the smallest average $\dot{V}O_2$ RMS error of 0.06 l/min. The corresponding parameter sets for each of the subjects are given in Table 6 and presented in Fig. 7.

In the validation we used the parameters resulting from the model fitting using Test 3 for the prediction of the $\dot{V}O_2$ consumption in the other tests. For the model simulation we used the measured power as input for the differential equations. We present the corresponding RMS prediction errors in Table 8.

Fig. 9 illustrates the modeling and prediction results for an example. We present the graphs of the $\dot{V}O_2$ model fitting, the prediction, and the measured $\dot{V}O_2$ against time for Test 4, where the subjects were self-pacing themselves. Note that the model prediction errors are mostly positive, i.e., the prediction overestimated the actual $\dot{V}O_2$ consumption, especially at times of severe

Table 6
Parameters of the fitted model for the subjects from Test 3.

Parameter Unit	$\dot{V}O_{2max}$ l/min	$\dot{V}O_{2base}$ l/min	s l/min/W	P_c W	V_Δ l/min	Δ W	T_1 min	τ_1 min	T_2 min	τ_2 min
Subject 1	5.91	1.14	10.2×10^{-3}	383	0.00	–	0:09.3	0:26.4	3:18.4	1:02.8
Subject 2	4.63	0.84	10.4×10^{-3}	243	0.63	29	0:04.2	0:25.5	3:04.4	5:00.0
Subject 3	3.85	0.56	10.4×10^{-3}	224	0.53	17	0:08.8	0:27.8	3:02.9	5:00.0
Subject 4	3.16	0.99	9.1×10^{-3}	217	0.14	28	0:07.7	0:29.7	1:08.6	1:05.6
Subject 5	4.87	0.98	10.3×10^{-3}	262	0.00	–	0:10.8	0:32.9	3:58.4	1:06.6

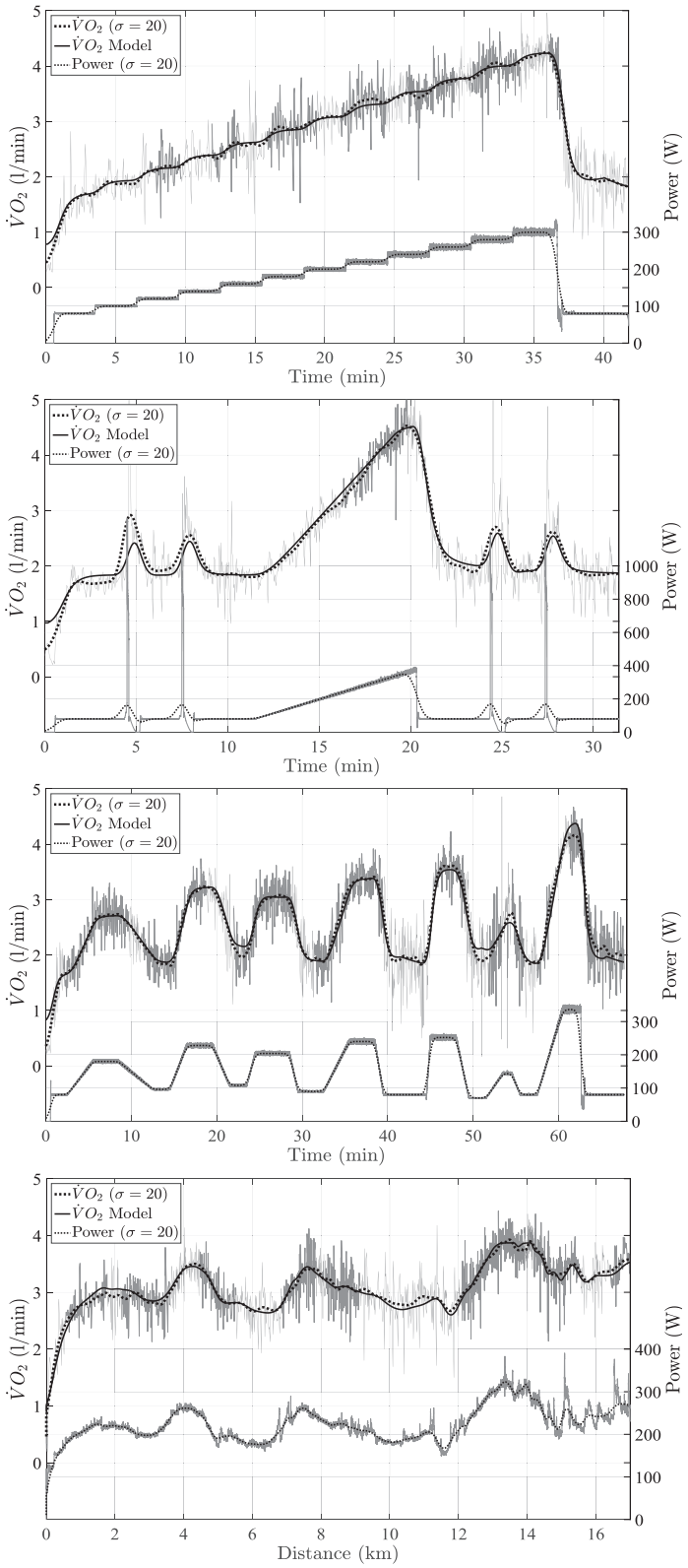

Fig. 8. $\dot{V}O_2$ fitting for Subject 2 on all four tests. The lower curves show the power, and the upper two parts depict the recorded and the best fitting $\dot{V}O_2$ curves. The noisy gray signals are the original (unfiltered) measurements.

Table 7
Errors of model fit. Parameters have been fitted for each case separately. The approximation quality is expressed by root-mean-square error (RMSE) and mean absolute percentage error (MAPE).

	Test 1		Test 2		Test 3		Test 4		Average	
	RMSE	MAPE	RMSE	MAPE	RMSE	MAPE	RMSE	MAPE	RMSE	MAPE
	l/min	%	l/min	%	l/min	%	l/min	%	l/min	%
Subject 1	0.08	2.3	0.25	7.3	0.11	3.1	0.08	1.8	0.13	3.6
Subject 2	0.05	2.0	0.14	5.2	0.10	3.5	0.07	2.3	0.09	3.2
Subject 3	0.04	1.8	0.08	3.2	0.05	2.1	0.07	2.3	0.06	2.3
Subject 4	0.07	2.7	0.10	4.2	0.17	4.9	0.08	2.4	0.10	3.6
Subject 5	0.05	1.7	0.13	4.1	0.09	3.3	0.09	1.8	0.09	2.7
Average	0.06	2.1	0.14	4.8	0.10	3.4	0.08	2.1	0.09	3.1

Table 8
Root-mean-square errors of model predictions for the three tests in the validation set.

	Test 1		Test 2		Test 4		Average	
	RMSE	MAPE	RMSE	MAPE	RMSE	MAPE	RMSE	MAPE
	l/min	%	l/min	%	l/min	%	l/min	%
Subject 1	0.24	5.5	0.50	12.6	0.40	9.3	0.38	9.1
Subject 2	0.25	7.3	0.21	7.6	0.49	14.3	0.31	9.7
Subject 3	0.14	5.7	0.19	8.3	0.31	8.5	0.21	7.5
Subject 4	0.32	9.4	0.19	7.3	0.18	5.2	0.23	7.3
Subject 5	0.30	9.0	0.19	5.5	0.67	17.0	0.38	10.5
Average	0.25	7.4	0.25	8.3	0.41	10.8	0.30	8.8

exercise intensity.

5. Discussion

Overall, the results show that in principle the approach to transferring the dynamic steady-state model from constant work rates to variable work rates was successful. Parameters could be estimated such that the measured $\dot{V}O_2$ data could be approximated with a small average RMS error of about 0.09 l/min, corresponding to a mean absolute percentage error of 3.1%. For model prediction the average error was around 0.30 l/min (MAPE of 8.8%).

An average RMS modeling error of only 0.09 l/min can be regarded as a very satisfactory result. The best one can expect from an optimal modeling is that the accuracy is in the range of the natural variability of the modeled quantities, and we show that this is the case here.

We were not able to locate comparable results on the variability of $\dot{V}O_2$ kinetics in the literature. Most reproducibility studies are limited to the investigation of the variability in $\dot{V}O_{2max}$ (Dideriksen & Mikkelsen, 2015; Katch, Sady, & Freedson, 1981; Thomas, Cunningham, Rechnitzer, Donner, & Howard, 1987). The few studies investigating the reproducibility of $\dot{V}O_2$ kinetics have demonstrated good measures of reproducibility only for parameters of on- and off-transient kinetics (Cannon, Schenone, & Kolkhorst, 2008; de Tarso Müller, Christofoletti, Zagatto, Paulin, & Neder, 2015; Kilding, Challis, Winter, & Fysh, 2005).

Therefore, we carried out an additional small study to investigate the reproducibility of $\dot{V}O_2$ kinetics for an incremental exercise protocol (unpublished work). In that study, 11 recreationally active subjects performed two identical cycling ramp tests to exhaustion on separate occasions. With the same metabolic unit and analytical methods as used in this study, we gathered $\dot{V}O_2$ measurements over the course of the ramp protocol. We obtained a grand average RMS difference between the $\dot{V}O_2$ measurements of the two tests of 0.09 l/min and a MAPE of 2.95%, which exactly matches our average RMS modeling error of 0.09 l/min.

We now compare our modeling and prediction results with our previous ones from Artiga Gonzalez et al. (2015). Both, modeling and prediction have been improved, which is illustrated with a typical case given by Test 4 of Subject 2. Fig. 10 shows the results of Artiga Gonzalez et al. (2015), to be compared with the new results in Fig. 9. In Fig. 10, two of the model parameters (critical power and maximal oxygen uptake) were set to pLT and $\dot{V}O_{2max}$ respectively, instead of being derived by means of the fitting procedure. Also, we increased the range for the time constant and the time delay of the second component and used the same smoothing ($\sigma = 20$) for both, power and $\dot{V}O_2$. In summary, with these changes on our revised method the precision of the model fit to the data is much better with 0.09 l/min versus 0.23 l/min and the predictions are a little better with a grand average of 0.30 l/min RMSE versus 0.37 l/min in Artiga Gonzalez et al. (2015).

Still, one cannot expect the modeling results to deliver precise estimates of physiological parameters like critical power or $\dot{V}O_{2max}$ or good estimates for the time constants. The parameters we obtain vary according to the training data. For example for critical

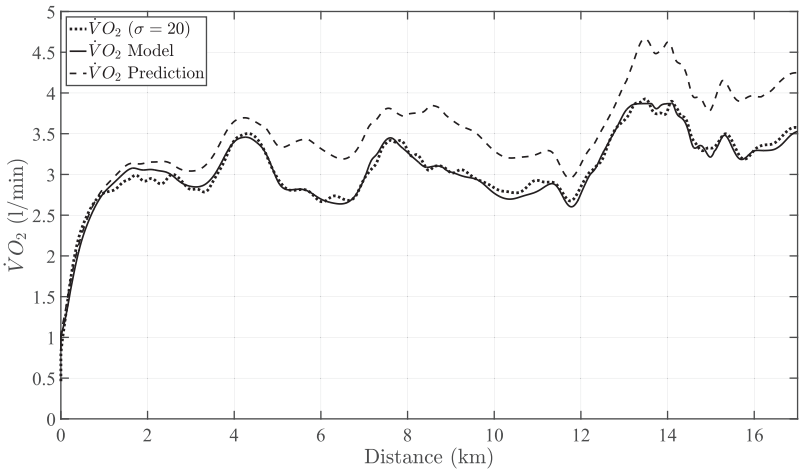

Fig. 9. Modeling and Prediction results for Test 4 of Subject 2. The RMS modeling error is 0.07 l/min, and the RMS prediction error, based on parameters trained with Test 3, is 0.49 l/min.

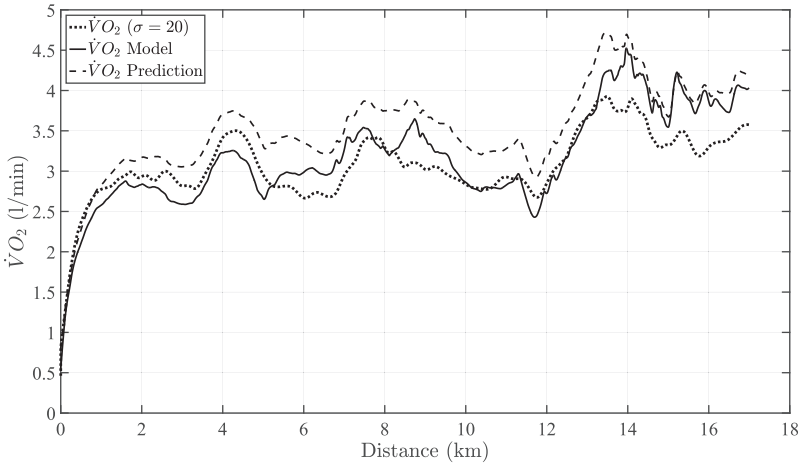

Fig. 10. Modeling and Prediction results as in the above Fig. 9, however with two of the model parameters (critical power and maximal oxygen uptake) set to the measured values instead of derived by means of the fitting procedure, see (Artiga Gonzalez et al., 2015) for details. The RMS modeling error is 0.35 l/min, and the RMS prediction error, based on parameters trained with Test 3, is 0.50 l/min. The model fit in our revised approach is much better (0.07 l/min) and the prediction a little better (0.49 l/min).

power, the average standard deviation within the four tests of one subject is 16 Watt. However, with a larger training data set consisting of tests like Test 3 or Test 4 we expect a better estimation of physiological parameters. The estimated time constants cannot be compared with the results derived by mono or double exponential fitting on constant work rate (Özyener et al., 2001) or by applying cross-correlation functions as in Hoffmann, Drescher, Benson, Rossiter, and Essfeld (2013), because our model does not consider the difference between on- and off-transient kinetics.

To illustrate and discuss the dynamics of the differential equation model for the oxygen dynamics, we provide Fig. 11 that illustrates the total oxygen consumption and the corresponding slow component, both with respect to the oxygen demand, $\dot{V}O_{2\text{base}} + A_1(P(t)) + A_2(P(t))$ and $A_2(P(t))$, respectively, and the modeled responses of the system, $\dot{V}O_2(t), x_2(t)$. Moreover, the corresponding oxygen consumption measurements as well as the applied power $P(t)$ are included. The exponential asymptotic dynamics for piecewise constant demands are clearly visible. Also note the delayed reaction, especially of the slow component. A large oxygen demand in the slow component may trigger a delayed overcompensation, leading to total $\dot{V}O_2$ estimates that are to too large, e.g., near $t = 50$ min.

A possible explanation of this artifact is that the slow component generally is not well understood yet, thereby having led to an inadequate steady state model upon which our model is based. This limits the dynamic phenomena that can be captured to those that are known and described in the literature. Moreover, some findings or assumptions about the type of functional dependencies are controversial, in particular regarding the slow component, see (Poole and Jones, 2012, page 953). For example, it is not clear at all that the slow component in constant work rate exercise tests at heavy and severe work rates is asymptotically exponential as expressed in Eq. (1) (Gaesser and Poole, 1996, pages 43, 44).

Therefore, instead of including the slow component one might conjecture that a dynamic model that discards the slow component

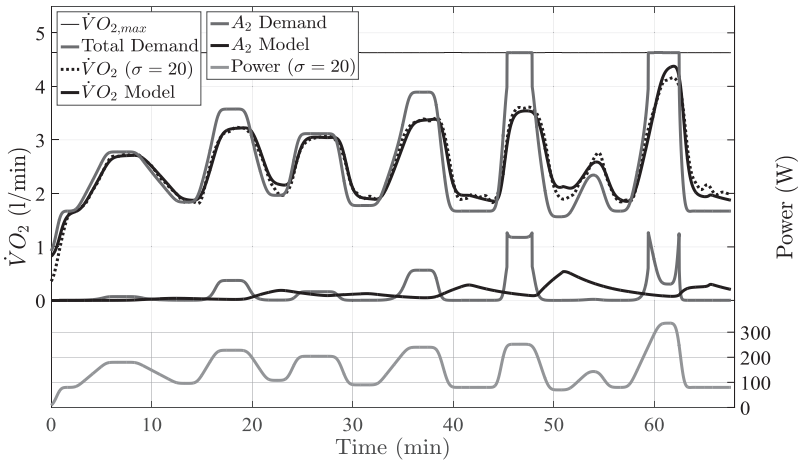

Fig. 11. Steady-state demand and dynamic model for Subject 2 on Test 3. See text for details.

would yield better prediction results. In Artiga Gonzalez et al. (2015) we checked this in a quick test by removing the slow component in the parameter fitting procedure. The results for prediction of Test 4 indicated a good improvement. However, for the other validation tests the predictions using the slow component were better. Still, this indicates that there is a good opportunity for improvements of the mathematical model beyond the direct transfer from constant to variable work rates.

6. Conclusions and future research

We contributed to the generalization of the commonly accepted model of the dynamics of oxygen uptake during exercise at constant work rates to variable load protocols by means of differential equations. We showed how the parameters in the model can be estimated and that the mathematical dynamical model can be used to predict the oxygen consumption for other load profiles. We found for five subjects and four very different test protocols (of up to about one hour in length) that on average the modeling RMS error of $\dot{V}O_2$ was 0.09 ± 0.03 l/min and the prediction RMS error in three tests was 0.30 ± 0.09 l/min.

An alternative approach to modeling would be to allow for different, more appropriate degrees of freedom in the mathematical model, again fitting the model type and parameters to empirical data, and calculating the model and prediction errors. For example, we could assume as above two additive model components (besides a constant baseline oxygen consumption) with different delay times and decay rates, however, with corresponding steady state oxygen demands that are restricted only by requiring (piecewise) monotonicity and that can be parametrized by a set of 10 parameters, the same number as in this paper. Moreover, as mentioned above, there is evidence for an asymmetry between on- and off-transient dynamics, i.e., the $\dot{V}O_2$ demand and time constants should be defined differently depending on whether the current $\dot{V}O_2$ value is below (on-transient case) or above the $\dot{V}O_2$ demand (off-transient case).

With such an approach, we expect a better data fitting. It remains an open question whether also the predictive power would be better than for our current model and whether the results could be interpreted in harmony with the current understanding of sport physiology and sport medicine.

Acknowledgment

This work has been supported by a research grant of the Deutsche Forschungsgemeinschaft (DFG) for the project “Powerbike – Model-based optimization for road cycling.”

We thank the anonymous reviewers for their very helpful comments and suggestions.

References

Artiga Gonzalez, A., Bertschinger, R., Brosda, F., Dahmen, T., Thumm, P.,, & Saupe, D. (2015). Modeling oxygen dynamics under variable work rate. *icSPORTS 2015: 3rd International congress on sport sciences research and technology support* (pp. 198–207). .

Baldari, C., & Guidetti, L. (2000). A simple method for individual anaerobic threshold as predictor of max lactate steady state. *Medicine and science in sports and exercise, 32*(10), 1798–1802.

Beaver, W. L., Wasserman, K., & Whipp, B. J. (1986). A new method for detecting anaerobic threshold by gas exchange. *Journal of Applied Physiology, 60*(6), 2020–2027.

Bishop, D., Jenkins, D. G., & Mackinnon, L. T. (1998). The relationship between plasma lactate parameters, wpeak and 1-h cycling performance in women. *Medicine and Science in Sports and Exercise, 30*(8), 1270–1275.

Cannon, D. T., Schenone, A., & Kolkhorst, F. W. (2008). On the reproducibility of oxygen uptake kinetics during heavy exercise. *The FASEB Journal, 22*, 1176–1178 (1MeetingAbstracts).

Cheng, B., Kuipers, H., Snyder, A., Keizer, H., Jeukendrup, A., & Hesselink, M. (1992). A new approach for the determination of ventilatory and lactate thresholds. *International Journal of Sports Medicine, 13*(07), 518–522.

Coyle, E. F., Martin, W. H., Ehsani, A. A., Hagberg, J. M., Bloomfield, S. A., Sinacore, D. R., & Holloszy, J. O. (1983). Blood lactate threshold in some well-trained

ischemic heart disease patients. *Journal of Applied Physiology, 54*(1), 18–23.
Dahmen, T. (2012). Optimization of pacing strategies for cycling time trials using a smooth 6-parameter endurance model. *Proceedings pre-olympic congress on sports science and computer science in sport (IACSS), Liverpool, England, UK, July 24–25*.
Dahmen, T., Byshko, R., Saupe, D., Röder, M., & Mantler, S. (2011). Validation of a model and a simulator for road cycling on real tracks. *Sports Engineering, 14*(2–4), 95–110.
de Tarso Müller, P., Christofoletti, G., Zagatto, A. M., Paulin, F. V., & Neder, J. A. (2015). Reliability of peak O 2 uptake and O 2 uptake kinetics in step exercise tests in healthy subjects. *Respiratory Physiology & Neurobiology, 207*, 7–13.
Dennis, S. C., Noakes, T. D., & Bosch, A. N. (1992). Ventilation and blood lactate increase exponentially during incremental exercise. *Journal of Sports Sciences, 10*(5), 437–449.
Dideriksen, K., & Mikkelsen, U. R. (2015). Reproducibility of incremental maximal cycle ergometer tests in healthy recreationally active subjects. *Clinical Physiology and Functional Imaging*.
Gaesser, G. A., & Poole, D. C. (1996). The slow component of oxygen uptake kinetics in humans. *Exercise and Sport Sciences Reviews, 24*(1), 35–70.
Heck, H., Mader, A., Hess, G., Mücke, S., Müller, R., & Hollmann, W. (1985). Justification of the 4-mmol/l lactate threshold. *International Journal of Sports Medicine, 6*(03), 117–130.
Hill, D. W. (1993). The critical power concept. *Sports Medicine, 16*(4), 237–254.
Hoffmann, U., Drescher, U., Benson, A., Rossiter, H., & Essfeld, D. (2013). Skeletal muscle $\dot{V}O_2$ kinetics from cardio-pulmonary measurements: assessing distortions through O_2 transport by means of stochastic work-rate signals and circulatory modelling. *European Journal of Applied Physiology, 113*(7), 1745–1754.
Jones, A. M., & Poole, D. C. (2005). Introduction to oxygen uptake kinetics and historical development of the discipline. In A. M. Jones, & D. C. Poole (Eds.). *Oxygen uptake kinetics in sport, exercise and medicine* (pp. 3–35). London: Routledge.
Katch, V. L., Sady, S. S., & Freedson, P. (1981). Biological variability in maximum aerobic power. *Medicine and Science in Sports and Exercise, 14*(1), 21–25.
Kilding, A., Challis, N., Winter, E., & Fysh, M. (2005). Characterisation, asymmetry and reproducibility of on-and off-transient pulmonary oxygen uptake kinetics in endurance-trained runners. *European Journal of Applied Physiology, 93*(5–6), 588–597.
Ma, S., Rossiter, H. B., Barstow, T. J., Casaburi, R., & Porszasz, J. (2010). Clarifying the equation for modeling of $\dot{V}O_2$ kinetics above the lactate threshold. *Journal of Applied Physiology, 109*(4), 1283–1284.
Martin, J. C., Milliken, D. L., Cobb, J. E., McFadden, K. L., & Coggan, A. R. (1998). Validation of a mathematical model for road cycling power. *Journal of Applied Biomechanics, 14*, 276–291.
MATLAB® (2017a). Global Optimization Toolbox™: User's Guide (R2017a). MathWorks®.
MATLAB® (2017b). MATLAB®: Mathematics (R2017a). MathWorks®.
Morton, R., Fukuba, Y., Banister, E., Walsh, M., Kenny, C. T., & Cameron, B. (1994). Statistical evidence consistent with two lactate turnpoints during ramp exercise. *European Journal of Applied Physiology and Occupational Physiology, 69*(5), 445–449.
Özyener, F., Rossiter, H. B., Ward, S. A., & Whipp, B. J. (2001). Influence of exercise intensity on the on-and off-transient kinetics of pulmonary oxygen uptake in humans. *The Journal of Physiology, 533*(3), 891–902.
Poole, D. C., & Jones, A. M. (2012). Oxygen uptake kinetics. Comprehensive. *Physiology, 2*, 933–996.
Stirling, J., Zakynthinaki, M., & Billat, V. (2008). Modeling and analysis of the effect of training on $\dot{V}O_2$ kinetics and anaerobic capacity. *Bulletin of Mathematical Biology, 70*(5), 1348–1370.
Svedahl, K., & MacIntosh, B. R. (2003). Anaerobic threshold: the concept and methods of measurement. *Canadian Journal of Applied Physiology, 28*(2), 299–323.
Thomas, S., Cunningham, D., Rechnitzer, P., Donner, A., & Howard, J. (1987). Protocols and reliability of maximal oxygen-uptake in the elderly. *Canadian Journal of Sport Sciences, 12*(3), 144–151.
Whipp, B. J., & Rossiter, H. B. (2005). The kinetics of oxygen uptake: Physiological inference from the parameters. In A. M. Jones, & D. C. Poole (Eds.). *Oxygen uptake kinetics in sport, exercise and medicine* (pp. 62–94). London: Routledge.
Whipp, B. J., Ward, S. A., Lamarra, N., Davis, J. A., & Wasserman, K. (1982). Parameters of ventilatory and gas exchange dynamics during exercise. *Journal of Applied Physiology, 52*(6), 1506–1513.